Inorg. Chem. **2009**, *48*, 3901−3903

Continuous Band-Gap Reduction on ZnO Submicrorods via Covering with $ZnS_{1-x}Se_x$ or $ZnSe_{1-x}Te_x$ Alloy in Core/Sheath Morphology

Yi-Zhi Huang,[†] Li-Ming Wu,[†,‡] Shao-Wu Du,[†] and Ling Chen*[,†]

State Key Laboratory of Structural Chemistry, Fujian Institute of Research on the Structure of Matter, Chinese Academy of Sciences, Fuzhou, Fujian 350002, People's Republic of China, and State Key Laboratory of Metastable Materials Science and Technology, Yanshan University, Qinhuangdao 066004, People's Republic of China

Received November 28, 2008

Submicrosized alloy cables of ZnO/w-$ZnS_{1-x}Se_x$ ($0 < x < 1$) and ZnO/s-$ZnSe_{1-x}Te_x$ ($0.8 \leq x < 1$) have been prepared. The lattice parameters of the sheath show linear compositional dependence following Vegard's law. The composition−band gap dependence follows the trend of $E_g^{ZnO/w\text{-}ZnS_{1-x}Se_x}(x) = 3.60 - 1.77x + 0.87x^2$ ($0.22 \leq x \leq 1$), $E_g^{ZnO/w\text{-}ZnS_{1-x}Se_x} = 3.25$ eV ($0 \leq x \leq 0.22$), and $E_g^{ZnO/s\text{-}ZnSe_{1-x}Te_x}(x) = 2.65 - 1.82x + 1.41x^2$ ($0 \leq x \leq 1$), respectively. The continuous band-gap modulations on ZnO-based heterostructures are associated with the core/sheath morphology and the nature of the sheath alloys.

Wide-band-gap II−VI semiconductor ZnO is the most interesting optoelectronic material for application in light-emitting laser diodes, solar cells, and photocatalysts.[1] Numerous works have been carried out to enhance the performance of these devices in order to obtain more emitting colors or to utilize wider solar light energies in both ultraviolet and visible regions. The band-gap reduction on ZnO-based materials is highly desired because a narrower gap allows low-energy absorptions and excitations. The commonly used strategy is to introduce an appropriate ion into ZnO as the dopant, of which the solubility limitation may unfortunately restrict the reduction extent. For example, a maximum narrowing of ~0.4 eV for a $Zn_{1-x}Cd_xO$ alloy may be restricted by the solubility of Cd^{2+} in ZnO (<16%)[2] and ~0.5 eV for $Zn_{1-x}Co_xO$ ($x = 0.10$) nanorods.[3]

The boron-chalcogen method is a facile pathway to synthesizing metal chalcogenides with considerable morphology controllability.[4,5] The core/sheath ZnO/ZnE cables thus-made exhibit type-I excitonic localization character; i.e., the electrons and holes are confined in either the core or the sheath only depending on their relative gap energies.[4] Their gap energies vary below that of ZnO (3.25 eV), for example, $E_g^{ZnO/ZnSe} = 2.65$ eV and $E_g^{ZnO/ZnTe} = 2.24$ eV, and the nature of the narrower band-gap component is responsible for the discrete band-gap reduction. These observations have led to an interesting question on the possibility of a continuous band-gap reduction on a ZnO/ZnE cable. The zinc chalcogenide alloy $ZnE_{1-x}E'_x$ may be a suitable sheath material for this purpose because the majority of the material is known to exhibit a narrower band gap than that of ZnO.[6] In this paper, we report the successful covering of $ZnS_{1-x}Se_x$ or $ZnSe_{1-x}Te_x$ alloys on ZnO submicrorods by a modified boron-chalcogen method. The thus-obtained ZnO/$ZnS_{1-x}Se_x$ ($0 < x < 1$) and ZnO/$ZnSe_{1-x}Te_x$ ($0.8 \leq x < 1$) alloy cables show continuous gap reductions in the ranges of 3.25−2.70 and 2.10−2.24 eV, respectively. The compositional dependence of the sheath−lattice parameter and the band gap−composition dependence of the alloy cable are discussed.

The ZnO/$ZnS_{1-x}Se_x$ or ZnO/$ZnSe_{1-x}Te_x$ alloy cables were synthesized via an external-to-internal consumption of ZnO with a modified method.[4] The majority of the template ZnO submicrorods were 100−800 nm in width and >5 μm in length. The reactions are described by eqs I and II.

$$3ZnO + 2B + 3(1 - x)S + 3xSe \rightarrow 3ZnS_{1-x}Se_x + B_2O_3 \quad \text{(I)}$$

$$3ZnO + 2B + 3(1 - x)Se + 3xTe \rightarrow 3ZnSe_{1-x}Te_x + B_2O_3 \quad \text{(II)}$$

The loading ratio of each reagent was ZnO:B:S/Se:Se/Te = 3:2:(1−x):x; note that the chalcogen was purposely loaded at $^1/_3$ of the stoichiometric amount to achieve an incomplete chalcogenation, by which the target ZnO/alloy cables were

* To whom correspondence should be addressed. E-mail: chenl@fjirsm.ac.cn. Tel.: (011)86-591-83704947. Fax: (011)86-591-83704947.
† Chinese Academy of Sciences.
‡ Yanshan University.

(1) (a) Pearton, S. J. *Wide Bandgap Semiconductors—Growth, Processing and Applications*; William Andrew Publishing: New York, 2000. (b) Bhargava, R. *Properties of Wide Bandgap II−VI Semiconductors*; INSPEC, The Institution of Electrical Engineers: London, 1997.
(2) (a) Wang, X. J.; Buyanova, I. A.; Chen, W. M.; Izadifard, M.; Rawal, S.; Norton, D. P.; Pearton, S. J.; Osinsky, A.; Dong, J. W.; Dabiran, A. *Appl. Phys. Lett.* **2006**, *89* (15), 151909. (b) Misra, P.; Sahoo, P. K.; Tripathi, P.; Kulkarni, V. N.; Nandedkar, R. V.; Kukreja, L. M. *Appl. Phys. A: Mater. Sci. Process.* **2004**, *78* (1), 37–40.
(3) Qiu, X. Q.; Li, L. O.; Li, G. S. *Appl. Phys. Lett.* **2006**, *88* (11), 114103.

10.1021/ic802280z CCC: $40.75
Published on Web 03/27/2009

thus generated. The ZnO/$ZnS_{1-x}Se_x$ cables were made in the entire range of $0 < x < 1$ ($x = 0.5$, 0.75, and 0.9 at 450 °C for 12 h; $x = 0.25$ at 600 °C for 12 h), while the ZnO/$ZnSe_{1-x}Te_x$ cables could only be obtained over a narrower range of $0.8 \leq x < 1$ ($x = 0.8$, 0.9) at 470 °C for 72 h. Any attempt with $x < 0.8$ below 750 °C could not produce the desired cables (higher temperature or longer reaction time would inevitably result in the deleterious destruction of the cable morphology). Such phenomena agree with the linear enthalpy−concentration dependence on a $ZnE_{1-x}E_x'$ alloy and are consistent with the fact that the mixing enthalpy in $ZnSe_{1-x}Te_x$ is systematically higher than that in $ZnS_{1-x}Se_x$ alloys.[7] Three end-point cables, ZnO/ZnS, ZnO/ZnSe, and ZnO/ZnTe, were also synthesized.

The phase identity was checked by X-ray diffraction (XRD) patterns taken on a PANalytical X'Pert PRO diffractometer. The diffraction peaks of the ZnO core of each alloy cable were used as internal standards to locate the peaks of the other coexistent phases. Elemental analysis was performed on a Vario EL III elemental analyzer for sulfur and on an Ultima-2 inductively coupled plasma optical emission spectrometer (ICP-OES) for selenium, tellurium, and zinc. The morphologies of the alloy cables were examined by a scanning electron microscope (SEM; JSF-6700F). The diffuse-reflectance spectra were recorded on a PerkinElmer Lambda-900 spectrophotometer.

Sharp peaks of wurtzite (w)-ZnO (JCPDS 36-1451) and the coexistent chalcogenide alloy are observed for each sample; two representatives are shown in Figure 1. The products are core/sheath cables, as shown in the insets in Figure 1. Detailed morphology characterizations on the end-point ZnO/ZnE cables have been previously reported.[4] As shown in Figure 1a, all of the diffraction peaks of $ZnS_{1-x}Se_x$ ($x = 0.5$) have been successfully indexed as wurtzite type. Compared with both the wurtzite ZnS (w-ZnS, JCPDS 36-1450) and the wurtzite ZnSe (w-ZnSe, JCPDS 15-0105), the peaks of the thus-made $ZnS_{1-x}Se_x$ show systematic position shifts. The microsized wurtzite-type $ZnS_{1-x}Se_x$ alloy reported here is rather unusual, because such a wurtzite structure had been found across the entire composition range only in nanosized materials or films[8a−c] but over a restricted range of x in the bulk form.[8d] The $ZnSe_{1-x}Te_x$ alloys ($x = 0.8$, 0.9) are successfully indexed as sphalerite-type (s) (Figure 1b).[9] The experimental elemental analyses show that the molar ratios of Se:(Se + S) in ZnO/$ZnS_{1-x}Se_x$ cables with $x = 0.25$, 0.5, 0.75, and 0.9 are 25.07, 50.02, 74.54, and 89.36%, respectively, and those of Te:(Te + Se) in ZnO/$ZnSe_{1-x}Te_x$ with $x = 0.8$ and 0.9 are 80.80 and 88.99%, respectively. These ratios are well consistent with the loaded ones, with deviations of no more than ±1%. The lattice parameters of w-$ZnS_{1-x}Se_x$ ($x = 0$, 0.25, 0.5, 0.75, 0.9) and s-$ZnSe_{1-x}Te_x$ ($x = 0$, 0.8, 0.9, 1) alloys are plotted against the composition in Figure 2. The lattice parameters of the sheath alloys show a linear dependence on the composition following Vegard's law, which is in good agreement with the previous reports.[8,9] Therefore, the formation of the homogeneous alloy sheath with the expected compositions on the ZnO core is concluded. Although at $x = 1$, the end-point ZnO/w-ZnSe cable could not be made under our experimental conditions, the extrapolation of the fitted line generates $a = 4.008$ Å and $b = 6.557$ Å for w-ZnSe (open circle and square in Figure 2a), being consistent with the JCPDS 15-0105 data ($a = 3.996$ Å and $b = 6.550$ Å).

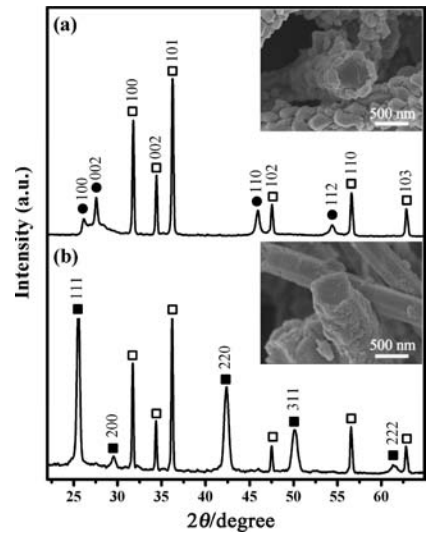

Figure 1. XRD patterns of the alloy submicrocables of (a) ZnO/w-$ZnS_{1-x}Se_x$ at $x = 0.5$ (●) and (b) ZnO/s-$ZnSe_{1-x}Te_x$ at $x = 0.8$ (■). □ indicates the diffraction peaks from w-ZnO. Insets are the corresponding SEM images.

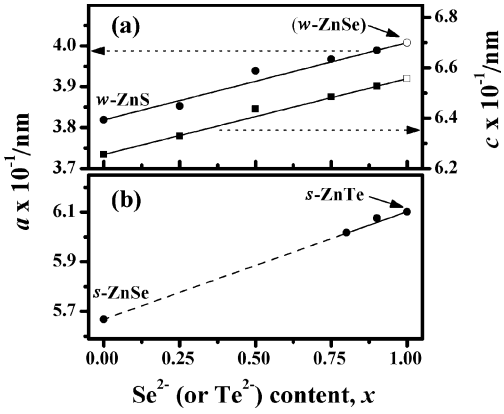

Figure 2. Composition dependence of the measured lattice parameters of (a) w-$ZnS_{1-x}Se_x$ and (b) s-$ZnSe_{1-x}Te_x$ alloy sheaths. ● and ■ represent the experimental a and c, respectively. ○ and □ are data for w-ZnSe from the extrapolation.

(4) Huang, Y. Z.; Chen, L.; Wu, L. M. *Inorg. Chem.* **2008**, *47* (22), 10723–10728.
(5) (a) Huang, Y. Z.; Chen, L.; Wu, L. M. *Cryst. Growth Des.* **2008**, *8* (2), 739–741. (b) Wu, L. M.; Seo, D. K. *J. Am. Chem. Soc.* **2004**, *126* (14), 4676–4681. (c) Wu, L. M.; Sharma, R.; Seo, D. K. *Inorg. Chem.* **2003**, *42* (19), 5798–5800.
(6) Larach, S.; Shrader, R. E.; Stocker, C. F. *Phys. Rev.* **1957**, *108* (3), 587.
(7) El Haj Hassan, F.; Amrani, B.; Bahsoun, F. *Phys. B* **2007**, *391* (2), 363–370.
(8) (a) Xu, H. Y.; Liang, Y.; Liu, Z.; Zhang, X. T.; Hark, S. K. *Adv. Mater.* **2008**, *20*, 3294–3297. (b) Wang, M.; Fei, G. T.; Zhang, Y. G.; Kong, M. G.; Zhang, L. D. *Adv. Mater.* **2007**, *19* (24), 4491–4494. (c) Kumar, V.; Sharma, T. P. *Opt. Mater.* **1998**, *10* (4), 253–256. (d) Christich, O. A.; Gorohova, E. I.; Mikhrin, S. B.; Rodnyi, P. A.; Potapov, A. S. *Phys. B* **2001**, *308−310*, 1201–1204.
(9) (a) Brasil, M. J. S. P.; Nahory, R. E.; Turco-Sandroff, F. S.; Gilchrist, H. L.; Martin, R. J. *Appl. Phys. Lett.* **1991**, *58* (22), 2509–2511. (b) ElNahass, M. M.; Khalifa, B. A.; ElRahman, A. M. A.; ElAriny, R. *Appl. Phys. A: Mater. Sci. Process.* **1996**, *63* (1), 81–86.

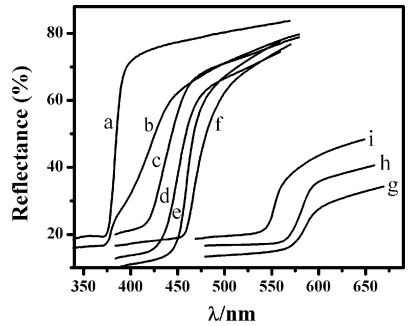

Figure 3. Diffuse-reflectance spectra of the cables of (a−e) ZnO/w-$ZnS_{1-x}Se_x$ ($x = 0$, 0.25, 0.5, 0.75, 0.9) and (f−i) ZnO/s-$ZnSe_{1-x}Te_x$ ($x = 0$, 0.8, 0.9, 1).

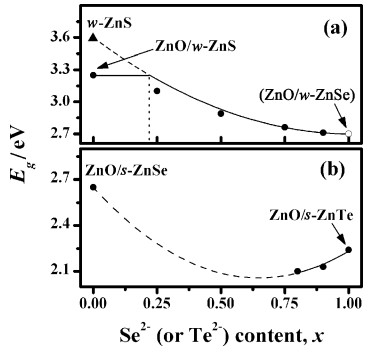

Figure 4. Compositional dependence of the band-gap energies of (a) ZnO/w-$ZnS_{1-x}Se_x$ and (b) ZnO/s-$ZnSe_{1-x}Te_x$ alloy cables. ● corresponds to the experimental data, ▲ represents the experimental gap for ZnS rods, and ○ represents the gap of w-ZnSe obtained from extrapolation of the curve.

The band-gap energies of the ZnO/alloy cables were determined by the diffuse-reflectance spectra (Figure 3). As expected, the ZnO/alloy cables exhibit type-I excitonic localization, and the alloy sheath on the ZnO rods generates a continuous gap reduction. The band-gap dependence on the composition of the sheath is discussed below.

The band gaps of $A_{1-x}B_xC$ alloys can be expressed by eq 1, which deviate considerably from the linear average.[7]

$$E_g^{A_{1-x}B_xC} = (1 - x)E_g^{Ac} + xE_g^{Bc} - bx(1 - x) \quad (1)$$

The quadratic coefficient b is the bowing parameter. For w-$ZnS_{1-x}Se_x$ and s-$ZnSe_{1-x}Te_x$ alloy sheaths, a quadratic fitting, as shown in Figure 4, generates eqs 2 and 3, respectively.

$$E_g^{ZnO/w-ZnS_{1-x}Se_x} = 3.60 - 1.77x + 0.87x^2 \quad (2)$$

$$E_g^{ZnO/s-ZnSe_{1-x}Te_x} = 2.65 - 1.82x + 1.41x^2 \quad (3)$$

The bowing parameters are 0.87 eV for w-$ZnS_{1-x}Se_x$ and 1.41 eV for s-$ZnSe_{1-x}Te_x$ alloy sheaths. The latter falls in the reported range of 1−1.62 eV for the bulk s-$ZnSe_{1-x}Te_x$ alloy,[9] and the former is larger than the reported range of 0−0.65 eV.[8] This deviation may be attributed to the extreme sensitivity of the band structure to bond deformations,[10] which may be related to the large lattice mismatch between the w-$ZnS_{1-x}Se_x$ alloy and w-ZnO (16−23%).

As the dashed curve in Figure 4a indicates, the gaps of w-$ZnS_{1-x}Se_x$ alloy sheaths in the range of $x < 0.22$ are wider than that of ZnO. According to type-I character, the band gap of such cables is therefore constant at 3.25 eV, as shown by the parallel solid line. Consequently, only in the range of $x < 0.22$, the gap−composition dependence of ZnO/w-$ZnS_{1-x}Se_x$ alloy cables differs from that of the simple $ZnS_{1-x}Se_x$ alloy. A continuous gap reduction from 3.25 to 2.70 eV of ZnO/w-$ZnS_{1-x}Se_x$ alloy cables has been realized under the condition of $x \geq 0.22$ (solid curve in Figure 4a).

As shown in Figure 4b, the solid curve indicates that the gap tuning between 2.10 and 2.24 eV on ZnO/s-$ZnSe_{1-x}Te_x$ alloy cables has been realized in the compositional range of $0.8 \leq x < 1$, while the experimental data in the range of $x < 0.8$ is not available at present (dashed curve in Figure 4b). Different from ZnO/w-$ZnS_{1-x}Se_x$, the band gaps of ZnO/s-$ZnSe_{1-x}Te_x$ cables are well below that of ZnO; hence, a larger degree of continuous reduction in the range of 2.06 (the minimum of the nonmonotonic function at $x \approx 0.65$) to 2.65 eV is suggested. In this paper, the observed maximum reductions on ZnO/w-$ZnS_{1-x}Se_x$ and ZnO/s-$ZnSe_{1-x}Te_x$ alloy cables are 0.55 and 1.15 eV, respectively, which is notably larger than what can be achieved by the introduction of Cd^{2+} or Co^{2+} dopant in ZnO.[3,4] The quadratic fitting shown in Figure 4b indicates a larger reduction of 1.19 eV for ZnO/s-$ZnSe_{1-x}Te_x$ at $x \approx 0.65$.

In conclusion, we have synthesized novel ZnO/alloy cables of ZnO/w-$ZnS_{1-x}Se_x$ ($0 < x < 1$) and ZnO/s-$ZnSe_{1-x}Te_x$ ($0.8 \leq x < 1$) via a modified boron-chalcogen method. The sheath−lattice parameters show linear compositional dependence following Vegard's law. The compositional dependence of the band-gap energy, determined by the diffuse-reflectance spectra, follows the trend of $E_g^{ZnO/w-ZnS_{1-x}Se_x}(x) = 3.60 - 1.77x + 0.87x^2$ ($0.22 \leq x < 1$), $E_g^{ZnO/w-ZnS_{1-x}Se_x} = 3.25$ eV ($0 \leq x \leq 0.22$), and $E_g^{ZnO/s-ZnSe_{1-x}Te_x}(x) = 2.65 - 1.82x + 1.41x^2$ ($0 \leq x \leq 1$) and shows the maximum reductions of 0.55 and 1.15 eV on ZnO/w-$ZnS_{1-x}Se_x$ and ZnO/s-$ZnSe_{1-x}Te_x$ alloy cables, respectively. Such continuous band-gap modulations on ZnO-based heterostructures are associated with the core/sheath morphology and the nature of the sheath alloys. This work provides a new approach for the band-gap reduction on ZnO-based materials, and a similar gap modification on other metal oxide semiconductors is highly possible.

Acknowledgment. Financial support by the National Natural Science Foundation of China under Projects 20521101, 20773130, 20733003, and 20803080, the 973 Program (2007CB815306), the "Key Project from Chinese Academe of Sciences, CAS" (Project KJCX2-YW-H01), the Knowledge Innovation Program of CAS, the State Key Laboratory Science Foundation (Grant 200808), and the "Key Project from Fujian Institute" (Project SZD07004).

IC802280Z

(10) James, B. E.; Alex, Z. *Phys. Rev. B* **1986**, *34* (8), 5992.